Angewandte Chemie
Eine Zeitschrift der Gesellschaft Deutscher Chemiker

Supporting Information

High-Performance Lithium–Air Battery with a Coaxial-Fiber Architecture

Ye Zhang[+], *Lie Wang*[+], *Ziyang Guo, Yifan Xu, Yonggang Wang, and Huisheng Peng**

anie_201511832_sm_miscellaneous_information.pdf

Supporting Information

Experimental section

Materials. Lithium wire and lithium sheet were obtained from Alfa Aesar. Lithium triflate ($LiCF_3SO_3$, 98%), tetraethylene glycol dimethyl ether ($C_{10}H_{22}O_5$, 99%), and N-methyl-2-pyrrolidinone (C_5H_9NO, 99%) were purchased from Aladdin Reagent. Trimethylolpropane ethoxylate triacrylate (average M_n of ~428), 2-hydroxy-2-methyl-1-phenyl-1-propanone ($C_6H_5COC(CH_3)_2OH$, 97%), and poly(vinylidene fluoride-co-hexafluoropropylene) (average M_n of ~130000) were purchased from Sigma-Aldrich. Heat shrinkable tube was provided by Suzhou Dasheng Materials Tech Co. Ltd. Commercial CNT films were purchased from Hengqiu Graphene Tech Co. Ltd.

Synthesis of spinnable carbon nanotube array. Spinnable carbon nanotube (CNT) arrays were synthesized by chemical vapor deposition with Fe (1.5 nm)/Al_2O_3 (5 nm) on a silicon substrate as the catalyst. Ethylene with a flowing rate of 90 sccm was used as the carbon source, and a gas mixture of argon (400 sccm) and hydrogen (30 sccm) was used as the carrier gas. The growth occurred at 740 ^oC for 10 min.

Characterization. The structures were characterized by scanning electron microscope (Hitachi FE-SEM S-4800 operated at 1 kV), transmission electron microscopy (JEOL, JEM-2100F), X-ray diffraction (Bruker AXS D8) and Fourier transform infrared spectrum (NICOLET 6700). X-ray photoelectron spectroscopy was recorded on an AXIS ULTRA DLD XPS System with MONO Al source (Shimadzu Corp.). Photoelectron spectrometer was recorded by using monochromatic Al KR radiation under vacuum at 5×10^{-9} Pa. All of the binding energies were referred to the C1s peak at 284.6 eV of the surface adventitious carbon. The photographs were taken by a camera (Nikon, J1).

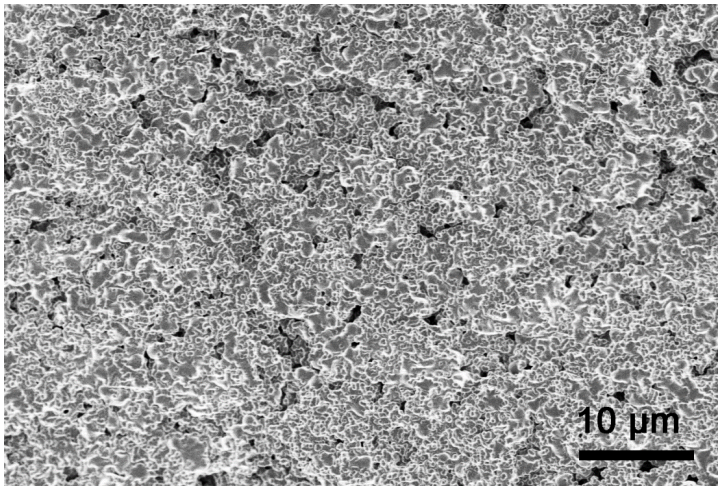

Figure S1. Scanning electron microscopy image of the gel electrolyte.

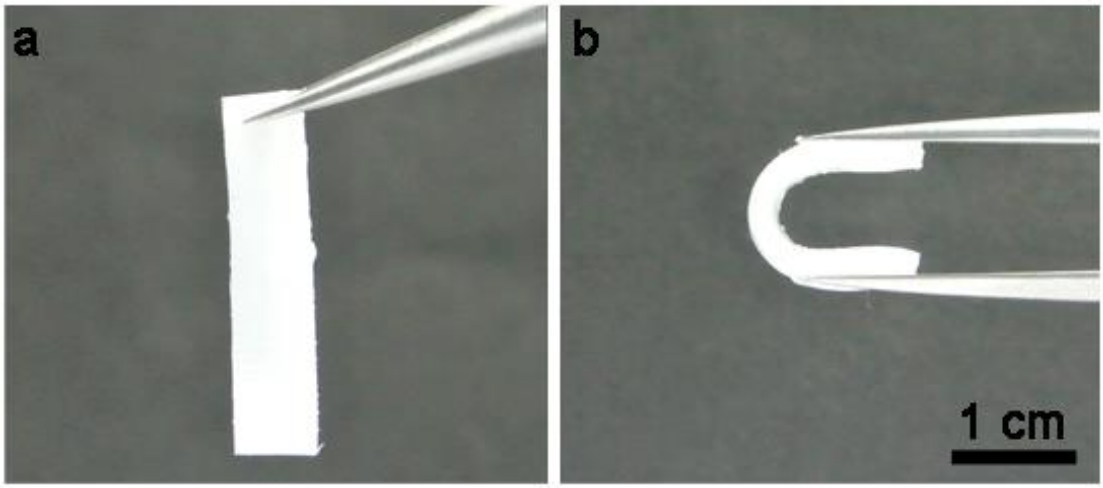

Figure S2. Photographs of the gel electrolyte before (**a**) and after (**b**) bending.

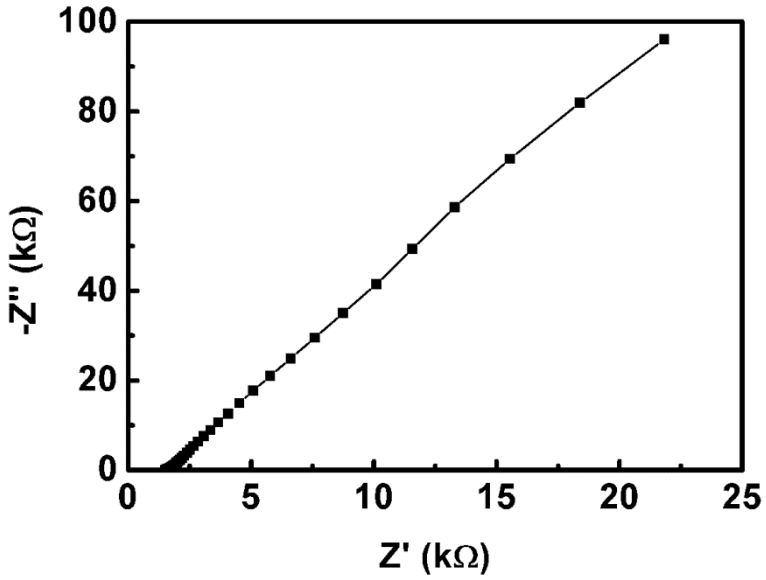

Figure S3. Electrochemical impedance spectroscopy of the gel electrolyte in the frequency ranging from 1 Hz to 100 kHz. Two parallel stainless steel sheets were inserted into the gel electrolyte with thickness of 1.1 cm and area of 0.63 cm^2. The tested electrolyte resistance of 1515 Ω was obtained from the intercept of the Nyquist plot with the real axis. Therefore, σ can be calculated as 1.15 mS/cm.

Figure S4. Photograph of a water drop on a Li sheet with (left) and without the coat of gel electrolyte (right).

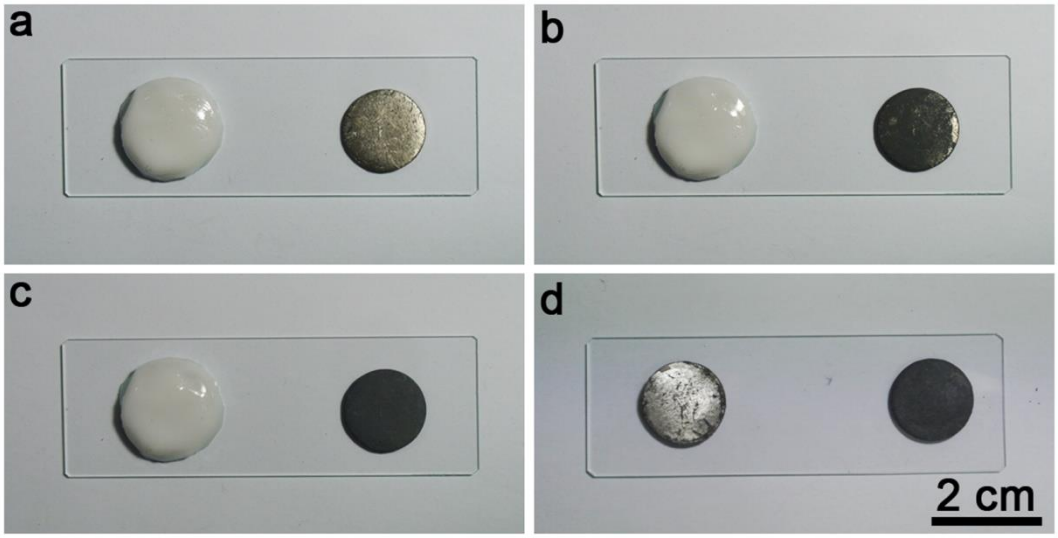

Figure S5. Photographs of a Li sheet with (left) and without the coat of gel electrolyte (right) before (**a**) and after exposure in air for 30 min (**b**) and 60 min (**c**). (**d**) The contrast of Li sheet with (left) and without (right) protection of gel electrolyte in air (relative humidity of 21.5%) for 60 min.

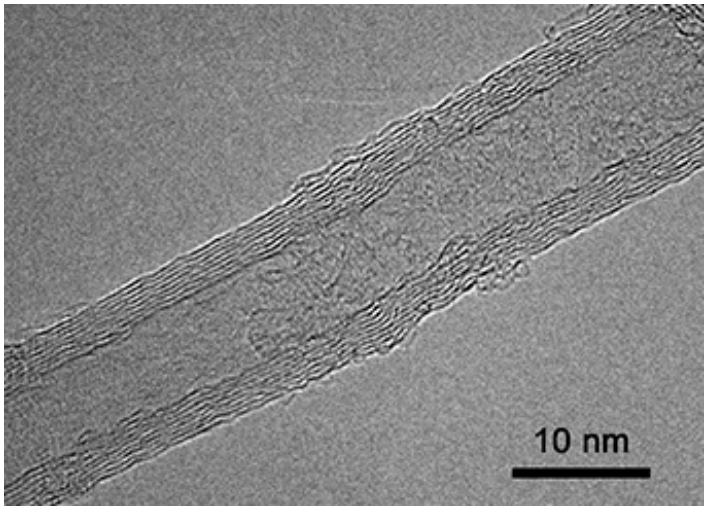

Figure S6. Transmission electron microscopy image of a CNT.

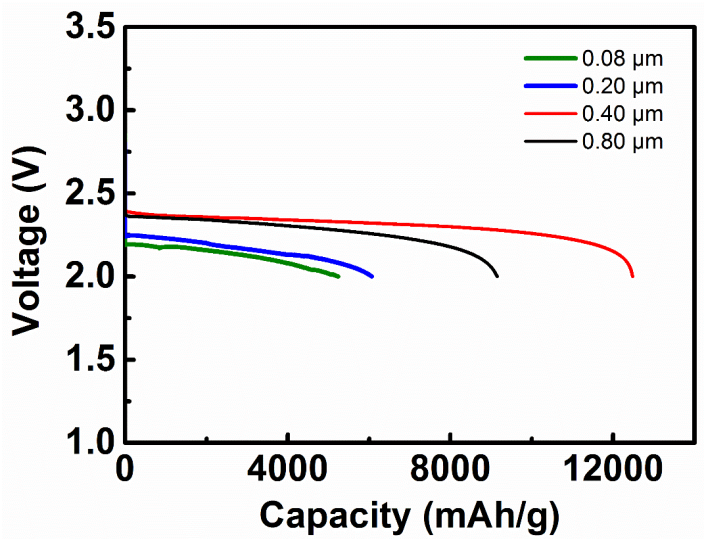

Figure S7. Galvanstatic discharge curves of the fiber-shaped Li-air batteries with different thicknesses of CNT layers at the same current density of 1400 mA/g.

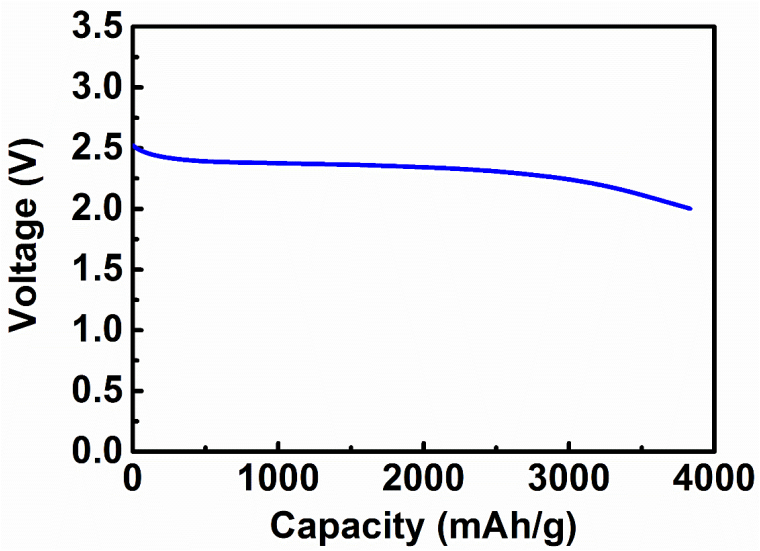

Figure S8. Galvanstatic discharge curves of a fiber-shaped Li-air battery with the commercial CNT film as air electrode.

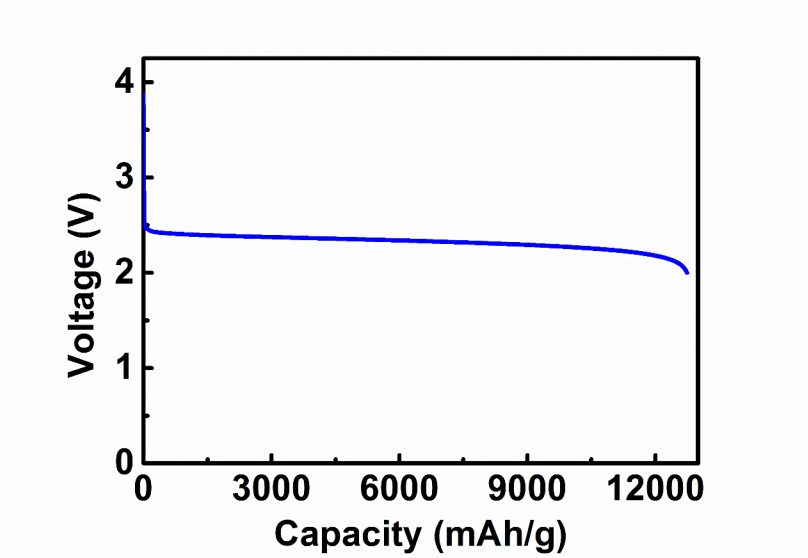

Figure S9. Galvanstatic discharge curve of a planar Li-air battery at a current density of 1400 mA/g. The batteries were constructed by the same electrolyte and cathode as the fiber-shaped Li-air battery.

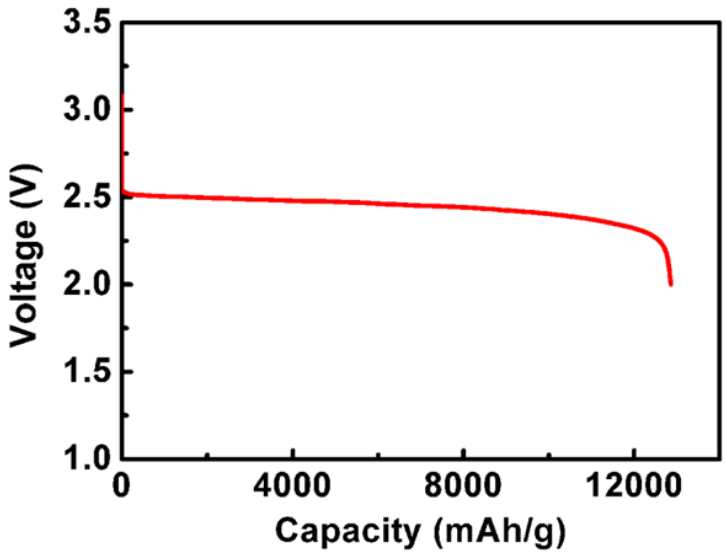

Figure S10. Galvanstatic discharge curve of the fiber-shaped Li-air battery at a current density of 350 mA/g.

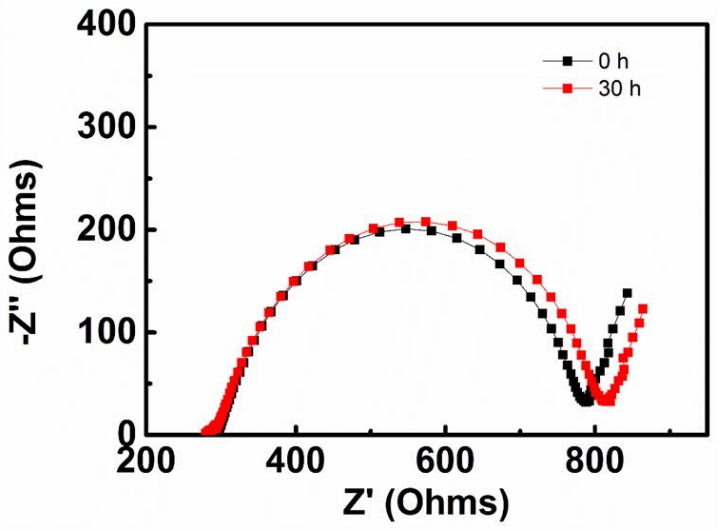

Figure S11. Time-dependence impedance spectra of the fiber-shaped Li-air battery.

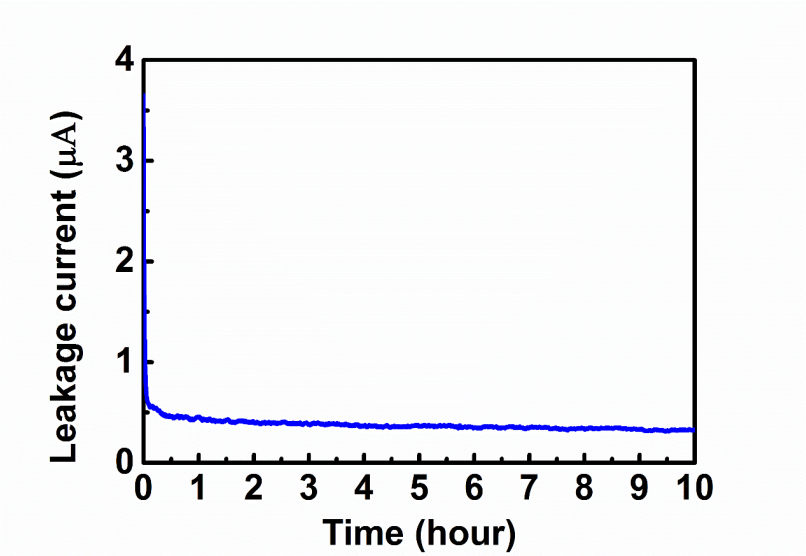

Figure S12. Leakage current measurement of the fiber-shaped Li-air battery.

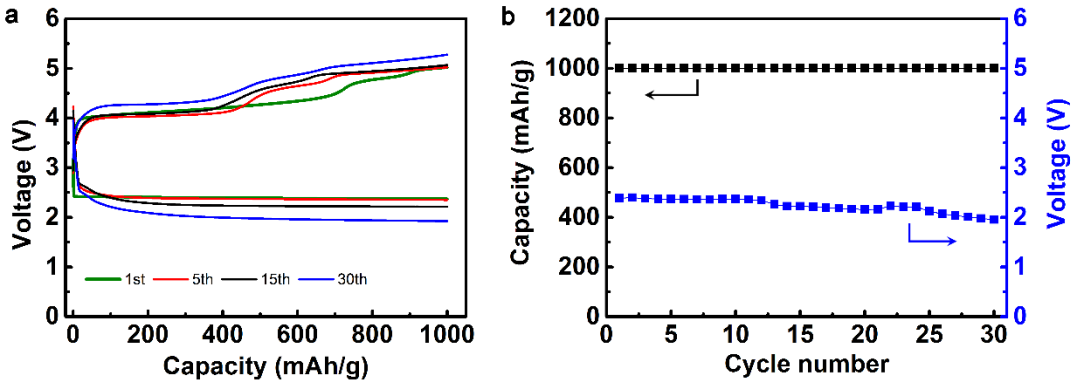

Figure S13. Charge and discharge curves **(a)** and the corresponding cycling performance **(b)** of the fiber-shaped Li-air battery at a current density of 1400 mA/g in air.

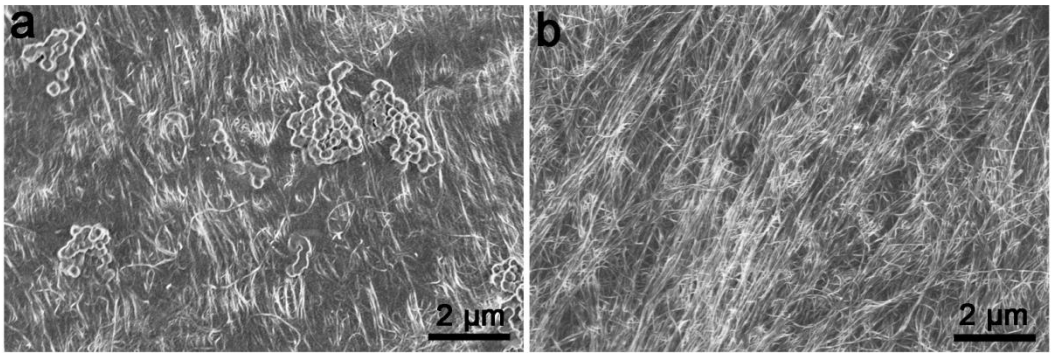

Figure S14. Scanning electron microscopy image of the CNT cathode after the first discharged **(a)** and first recharged **(b)**.

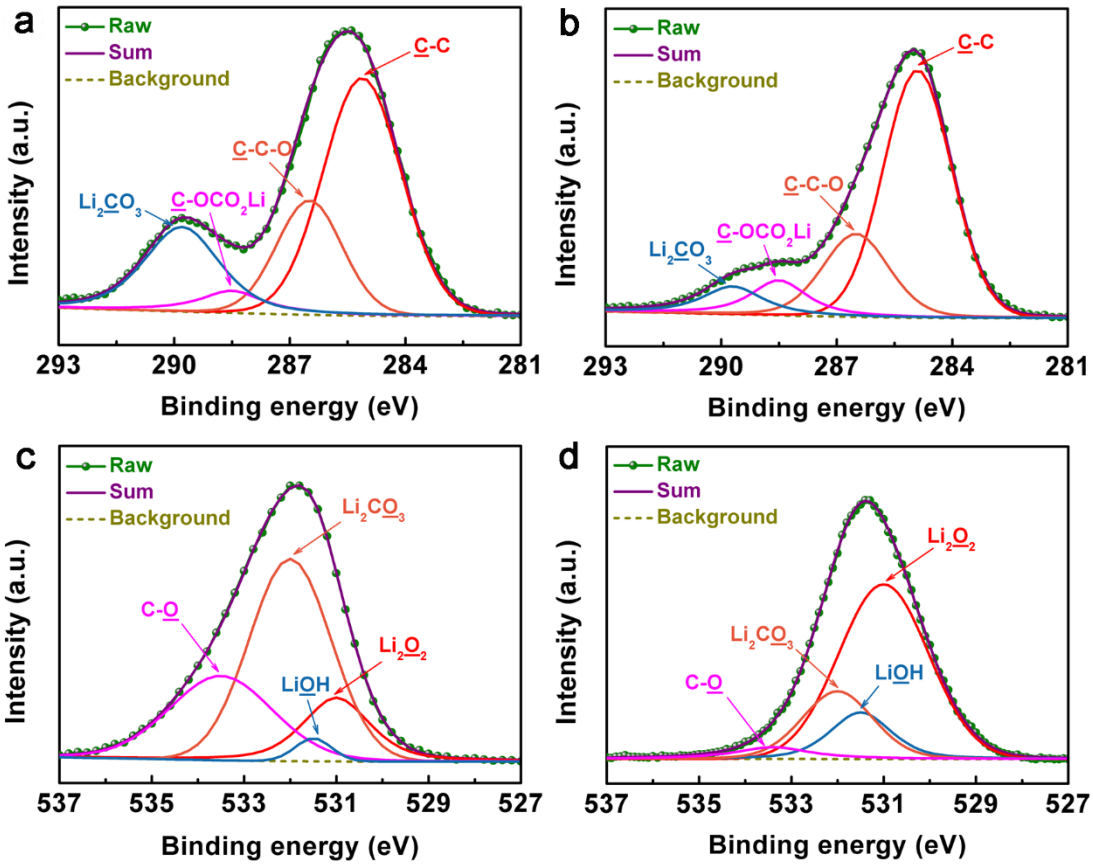

Figure S15. X-ray photoelectron spectroscopy C1s and O1s signals of the CNT cathode after the 5th discharge in air **(a, c)** and pure O_2 **(b, d)**.

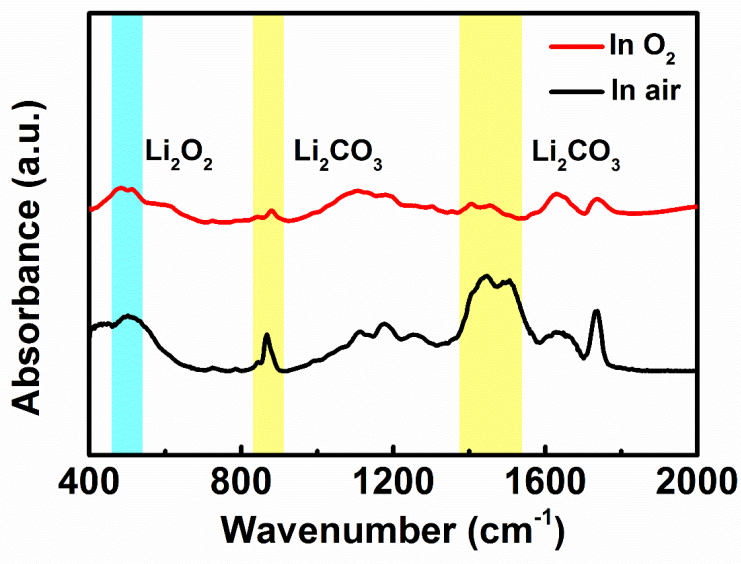

Figure S16. Fourier transform infrared spectra of the CNT cathode after the 5th discharge in air and pure O_2.

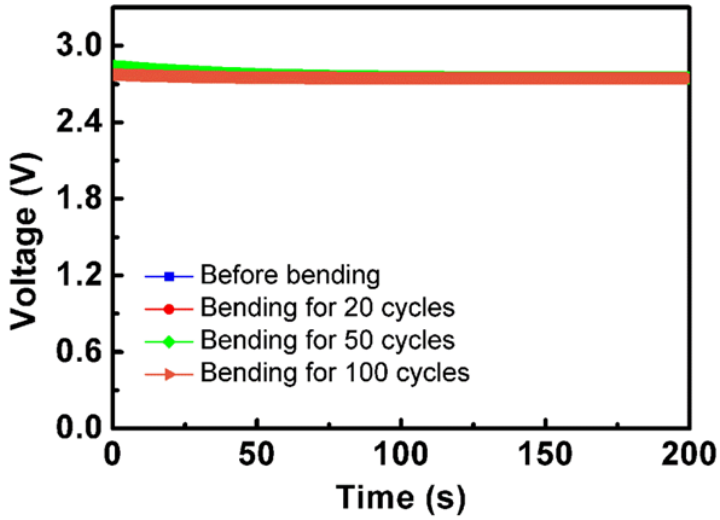

Figure S17. Discharge curves of a fiber-shaped Li-air battery before and after bending for 20, 50 and 1000 cycles with a bending angle of 90 °. The measurements were performed at a current density of 350 mA/g.